Catal Lett (2012) 142:1026–1032
DOI 10.1007/s10562-012-0849-6

Efficient Removal of Toxic Pollutants Over Fe–Co/ZrO_2 Bimetallic Catalyst with Ozone

Yulun Nie · Shengtao Xing · Chun Hu · Jiuhui Qu

Received: 7 March 2012 / Accepted: 28 May 2012 / Published online: 19 June 2012

Abstract Fe–Co bimetallic oxides supported on mesoporous zirconia (Fe–Co/ZrO_2) was prepared using incipient wetness co-impregnation method and characterized by transmission electron microscopy, X-ray diffraction, X-ray photoelectron spectroscopy and UV–vis diffuse reflectance spectra. Compared with individual component Fe or Co catalysts, Fe–Co/ZrO_2 exhibited higher ozonation efficiency for the degradation of the tested toxic pollutants, as demonstrated with the herbicides 2,4-dichlorophenoxyacetic acid and pharmaceutical phenazone, diphenhydramine hydrochloride in aqueous solution. Furthermore, the characterization studies indicated that Fe–Co oxides were highly dispersed on the surface of mesoporous zirconia with multivalent oxidation states. The interfacial electron transfer process was greatly enhanced due to the presence of two redox couples (Fe^{3+}/Fe^{2+} and Co^{2+}/Co^{3+}) in Fe–Co/ZrO_2, which caused the higher catalytic reactivity for ozone decomposition into $^{\bullet}OH$ radicals, leading to the efficient removal of toxic pollutants in aqueous solution. The catalytic mechanism of pollutants degradation over Fe–Co/ZrO_2 with ozone was proposed on the basis of all information obtained under different experimental conditions.

Keywords Bimetallic catalyst · Ozonation · Toxic pollutants · Removal · Mechanism

Electronic supplementary material The online version of this article (doi:10.1007/s10562-012-0849-6) contains supplementary material, which is available to authorized users.

Y. Nie · S. Xing · C. Hu (✉) · J. Qu
State Key Laboratory of Environmental Aquatic Chemistry, Research Center for Eco-environmental Sciences, Chinese Academy of Sciences, Beijing 100085, China
e-mail: huchun@rcees.ac.cn

1 Introduction

The increasing worldwide contamination of freshwater with thousands of industrial and natural chemicals is a major environmental problem facing humanity. Although most of these compounds are present at low concentrations, many of them raise considerable toxicological concerns, particularly when present as components of complex mixtures [1]. The ozonation has been used worldwide as an effective way to achieve degradation of many contaminants during drinking water treatment [2]. However, some compounds are relatively refractory to ozonation treatment due to the selective reactions of ozone. Heterogeneous catalytic ozonation was then developed to enhance the production of hydroxyl radicals ($^{\bullet}OH$) and overcome the limitations of ozonation processes [3, 4]. Supported and unsupported metals and metal oxides are the most commonly tested catalysts for the ozonation of organic compounds in water [5–8]. Experimental results indicate that the removal efficiencies of pollutants are significantly enhanced in the presence of catalysts compared to ozone alone.

Bimetallic nanoparticle catalysts occupy a position of high prominence in modern heterogeneous catalysis. The mixed oxides were capable of mutual interactions and the activity was usually higher than that of their individual components [9–11]. Published reports revealed that enhance catalytic performance apparently arise from the synergy between the component elements at the nanoscale which is absent in solid solutions of the two bulk metals [12, 13]. Although various combinations of bimetallic nanoparticles have been widely used for reactions of petrochemical significance (such as Fisher-Tropsch synthesis) [14] and degradation chlorinated organic compounds [11, 15], catalytic ozonation of toxic pollutants in water using these nanoparticles remains an unexplored area.

Recently, evidence had been obtained that the dispersed active species on support showed efficient catalytic performance. It was reported that the outstanding activity of CuO–MO/CeO_2–Al_2O_3 was attributed to the formation of well-dispersed and highly reducible metal oxides species over the catalyst surface [16]. Liu [17] attributed the high activity of CuO–CoO_x/$Ce_{0.67}Zr_{0.33}O_2$ to the synergistic effect between the dispersed copper and cobalt oxide on the surface of the support. The structure and dispersion of the supported metal oxide depend primarily on the preparation method, the nature of the support, and the type of precursor itself. Ordered mesoporous materials, with their intrinsically high surface areas, are particularly suitable for this purpose.

Herein, Fe–Co binary metal oxides supported on mesoporous zirconia was prepared via incipient wetness co-impregnation method. The catalyst exhibited higher ozonation efficiency for the degradation of the tested toxic pollutants than that of monometallic Fe or Co catalysts. This was mainly contributed to the multivalent oxidation states, high dispersion of Fe–Co oxides and the enhanced interfacial electron transfer process. The catalytic mechanism of pollutants degradation over Fe–Co/ZrO_2 with ozone was also discussed based on all the experimental results.

2 Experimental

2.1 Materials

Zirconium oxychloride, iron nitrate nonahydrate, cobalt nitrate hexahydrate were purchased from the Yili Company. Triblock copolymer $(EO)_{20}(PO)_{70}(EO)_{20}$(P123) was purchased from Sigma-Aldrich. 2,4-dichlorophenoxyacetic acid (2,4-D), phenazone (PZ), diphenhydramine hydrochloride (DP) were purchased from Acros. All reagents used in this work were analytical grade and used without further purification. All solutions were prepared with deionized water. The solution pH was adjusted by a diluted aqueous solution of NaOH or HCl.

2.2 Catalyst Preparation

According to a previous work [18], mesoporous zirconia (ZrO_2) was prepared via solid-state reaction using the structure-directing method. The bimetallic Fe–Co and monometallic Fe, Co catalysts supported on ZrO_2 were prepared by incipient wetness co-impregnation method. Aqueous solution of $Fe(NO_3)_3{\cdot}9H_2O$ and/or $Co(NO_3)_2{\cdot}6H_2O$ with different Fe/Co atomic ratio was added into dry ZrO_2 powder. After impregnation for 24 h, the sample was dried at 383 K for several hours and then cooled and washed with deionized water. The sample was dried at 383 K for several hours and finally calcined in a muffle furnace (exposed to static air) at 623 K for 2 h at a heating rate of 5°/min. The resulting catalysts were labeled as Fe–Co/ZrO_2.

2.3 Catalyst Characterization

TEM images of the catalyst were examined using a TEM Hitachi H-7500. The X-ray powder diffraction (XRD) patterns of the catalysts were recorded on a Scintag-XDS-2000 diffractometer with Cu Kα radiation ($\lambda = 1.54059$ Å). The X-ray photoelectron spectroscopy (XPS) data were taken on an AXIS-Ultra instrument from Kratos using monochromatic Al Kα radiation (225 W, 15 mA, 15 kV) and low-energy electron flooding for charge compensation. To compensate for surface charge effects, the binding energies were calibrated using the C_{1s} hydrocarbon peak at 284.80 eV. UV–vis diffuse reflectance spectra of the samples were recorded on a UV–vis spectrophotometer (Hitachi UV-3900) with an integrating sphere attachment for their reflectance in the range of 200–800 nm and $BaSO_4$ was the reflectance standard.

In situ ATR-FTIR spectroscopy. To prepare an ATR sample, a desired amount of Fe–Co/ZrO_2 was added into water or ozone solution with/without PO_4^{3-} and then sonicated. A short time before running the spectra, the samples were centrifuged; half of the supernatant was used as reference, the solid resuspended in the other half was used as the sample. This procedure yielded a solid concentration of 100 g L^{-1}. The ATR-FTIR spectra were recorded using a Tensor 27 infrared spectrometer with a DLaTGS detector and a ZnSe horizontal ATR cell. Infrared spectra over the 4,000–650 cm^{-1} range were obtained by averaging 32 scans with a resolution of 4 cm^{-1} at room temperature. The spectrum of Fe–Co/ZrO_2 in suspension was the result of subtracting the spectrum of the supernatant (reference) from the spectrum of the slurry (sample). The cell remains in place throughout the running of every single-beam spectra of the empty cell, reference, and sample so that its transmittance and average angle of incidence are constant.

2.4 Procedures and Analysis

Batch experiments were carried out with a 1.2-L reactor. The reaction temperature was maintained at 20 °C. In a typical experiment, 1 L of aqueous suspensions (pH = 7.0) of pollutants and 2.0 g of catalyst powders were placed in the reactor. The suspension was continuously magnetically stirred and 30 mg gaseous O_3/L oxygen-ozone was bubbled into the reactor through the porous plate of the reactor bottom at a 12 L h^{-1} flow rate. The ozone was generated

by a 3S-A5 laboratory ozonizer (Tonglin Technology, China) and pumped into the reactor. Samples were taken at given time intervals (the residue O_3 was quenched by the addition of an aliquot of 0.1 M $Na_2S_2O_3$) and filtered through a millipore filter (pore size 0.45 μm) to remove particles. The filtrates were analyzed by TOC removal with a Phoenix 8000 TOC analyzer. The gas ozone was determined by KI method (iodometry method). The aqueous ozone concentration was determined with the indigo method [19].

3 Results and Discussion

3.1 Catalytic Ozonation Efficiency of Different Catalysts

The catalytic activities of Fe–Co/ZrO_2 with different Fe/Co atomic ratio were evaluated by catalytic ozonation of 2,4-D at neutral pH. As shown in Fig. 1, only 19 % of TOC was removed at a reaction time of 20 min in the presence of ozone alone, while the TOC removal increased greatly with the addition of different catalyst. Moreover, with the amount of iron oxide in Fe–Co/ZrO_2 increasing, the TOC removal efficiency increased and reached a certain value at Fe/Co atomic ratio = 1:1 and the TOC content of the 2,4-D solution was rapidly and greatly reduced by 94 %. And the TOC removal efficiency decreased at Fe/Co atomic ratio = 2:1. The results suggested that the Fe/Co atomic ratio existed an optimum value and the synergistic effect between Fe–Co oxides played a crucial role in the enhancement of Fe–Co/ZrO_2 catalytic activity. Fe–Co/ZrO_2 (Fe/Co = 1:1, the actual value was 3:1 in the catalyst by EDX analysis) was then used for all the experiments unless otherwise specified. Moreover, the maximum amount of Fe^{3+} and Co^{2+} in solution during the ozonation process was 0.042 and 0.015 mg/L by ICP technique. This indicated that Fe–Co/ZrO_2 was stable enough and was appropriate for use as a heterogeneous ozonation catalyst.

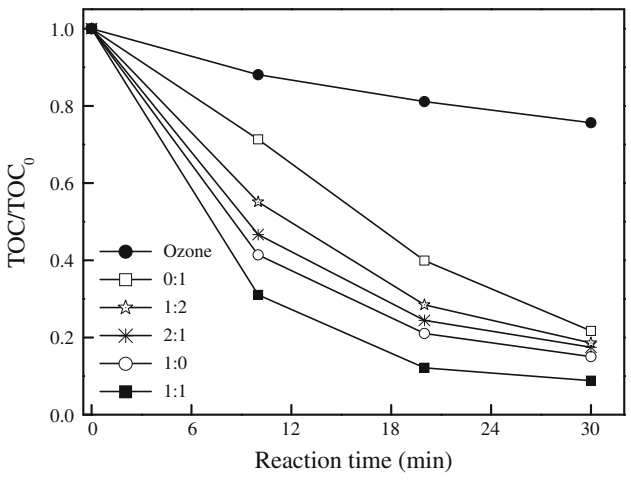

Fig. 1 Degradation of 2,4-D (50 mg/L) with ozone over Fe–Co/ZrO_2 with different Fe/Co atomic ratio (pH = 7.0, catalyst = 2.0 g/L, gas ozone concentration = 30 mg/L)

3.2 Characterization of Fe–Co/ZrO_2

TEM images (Fig. 2) suggested that iron and cobalt oxide was successfully supported on the surface of ZrO_2 and ZrO_2 still had an ordered meso-structure. Figure 3 showed the XRD patterns and BET analysis of ZrO_2 and Fe–Co/ZrO_2. In comparison with ZrO_2, no XRD diffraction peaks of iron and cobalt oxide were observed in the sample. There was also no significant change of BET area and distribution of pore diameter whether the iron and cobalt were introduced or not. The results indicated that iron and cobalt oxide was incorporated in the structure of ZrO_2 with high dispersion and smaller particle sizes.

Fe–Co/ZrO_2 was further characterized by XPS and UV–vis DRS to affirm the metallic state of iron and cobalt. As shown in Fig. 4, the peaks at 711, 718, and 725 eV represented the binding energies of $Fe2p_{3/2}$, shake-up satellite $Fe2p_{3/2}$, and $Fe2p_{1/2}$, respectively, suggesting the existence of Fe_2O_3 or FeOOH [20, 21]. The metallic state of Co could not be confirmed by XPS measurement may be due to its lower content and high dispersion [22]. However, the metallic state of Co could be measured semiquantitatively by UV–vis DRS. As shown in Fig. 5 (inset), Fe–Co/ZrO_2 exhibited a great light absorption due to the color of the catalyst, indicating the presence of iron or cobalt oxide. The relative UV–vis absorption spectrum of Fe–Co oxides was different spectrum from that of Fe–Co/ZrO_2 and ZrO_2. The peaks at 287 and 459 nm were attributed to cobalt in octahedral environment, in which the former could be assigned to charge transition and the latter to $^5T_{2g} \rightarrow {}^5E_g$ transition [23, 24]. The absorption shoulder between 300 and 400 nm was attributed to electronic transition of Co^{3+} in disordered tetrahedral environment [23]. Moreover, the peak at 425 nm also indicated that Co_3O_4 was formed in a very small amount [25]. The results indicated that iron and cobalt oxide mainly existed as multivalent mixtures on the surface of ZrO_2.

3.3 Performance of Fe–Co/ZrO_2 Under Different Conditions with Ozone

Figure 6 showed the TOC removal of different pollutants in Fe–Co/ZrO_2 suspensions with ozone. Both DP and PZ were degraded efficiently as 2,4-D and the TOC removal ratio followed the order 2,4-D > PZ > DP. The results indicated the Fe–Co/ZrO_2 catalyst was highly effective for

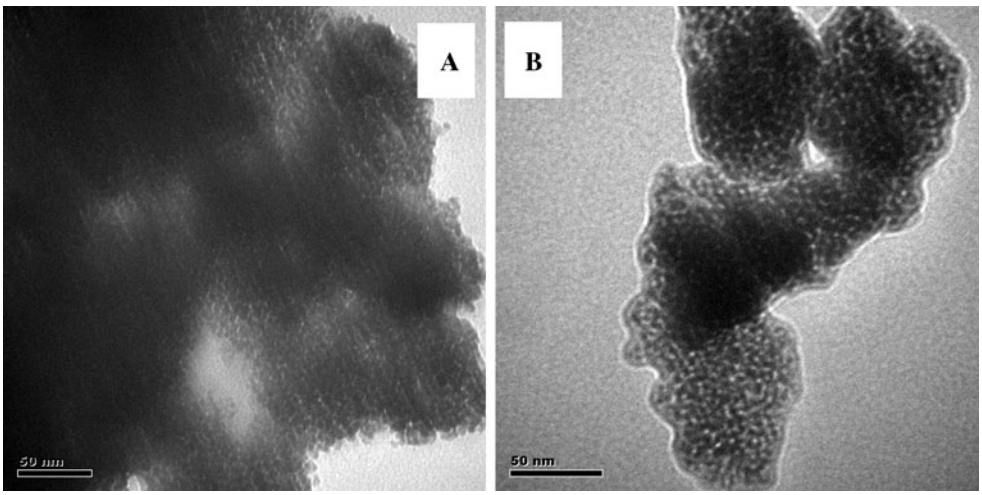

Fig. 2 TEM images of Fe–Co/ZrO_2

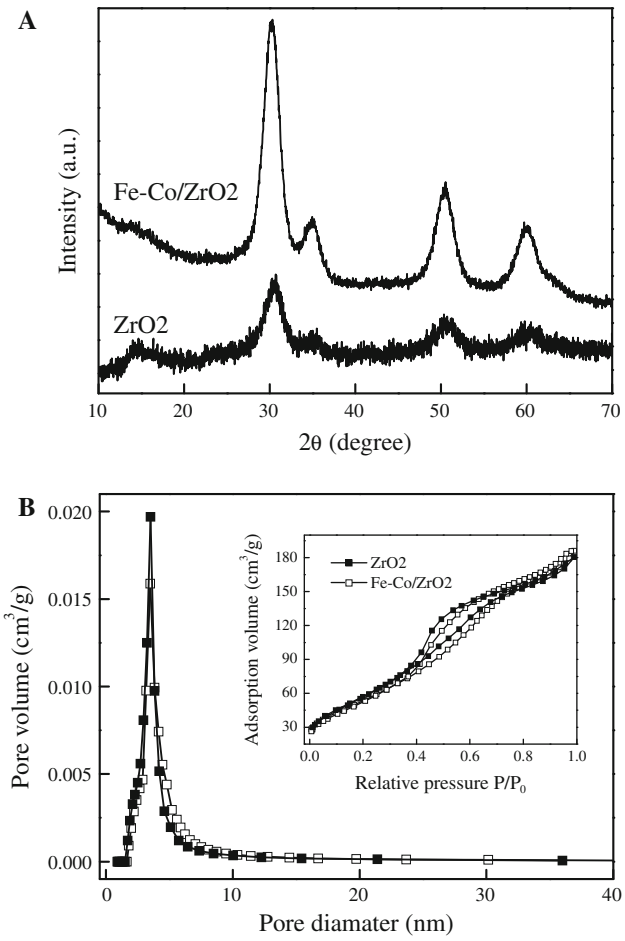

Fig. 3 XRD patterns and BET analysis of different catalyst

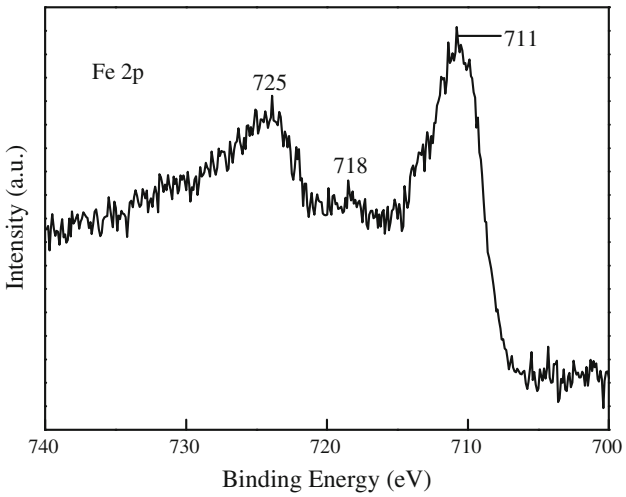

Fig. 4 XPS spectrum of Fe2p in Fe–Co/ZrO_2

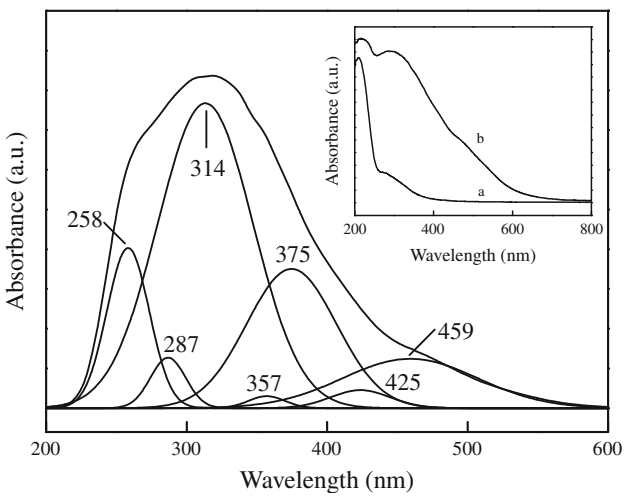

Fig. 5 Deconvoluted subbands of Fe–Co oxides. Inset showed the diffuse reflectance UV–vis spectra of *a* ZrO_2, *b* Fe–Co/ZrO_2

the mineralization of different pollutants in the aqueous solution.

Furthermore, the catalyst exhibited high efficiency for the degradation of 2,4-D at pH 4.0–7.0 (inset of Fig. 7). As

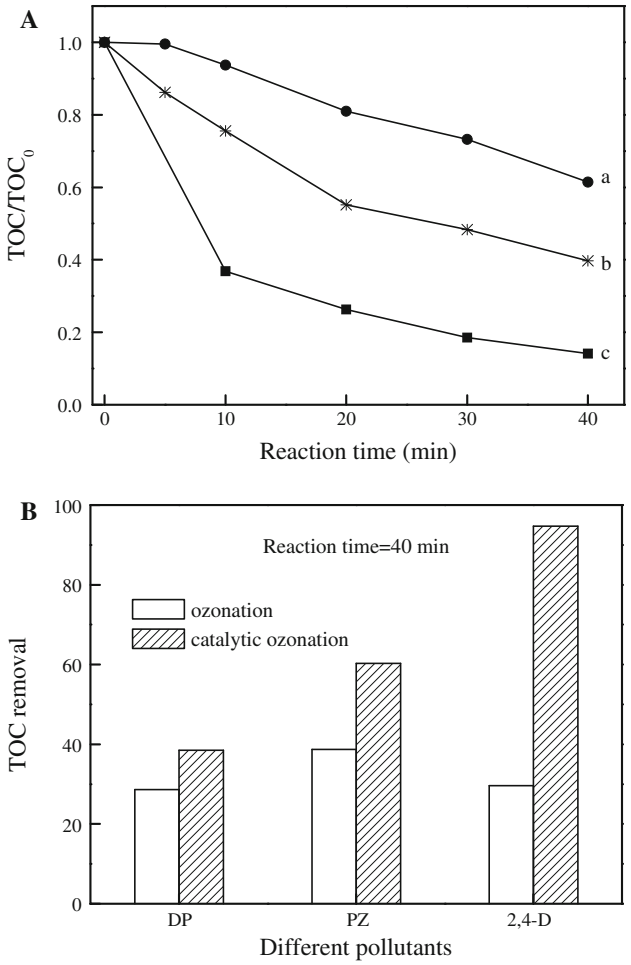

Fig. 6 **a** TOC removal during the degradation of different pollutants (50 mg/L) in aqueous dispersions of Fe–Co/ZrO_2 with ozone: *a* DP, *b* PZ, *c* 2,4-D; **b** TOC removal of different pollutants in ozonation and catalytic ozonation over Fe–Co/ZrO_2. (pH = 7.0, catalyst = 2.0 g/L, gas ozone concentration = 30 mg/L)

shown in Fig. 7, Fe–Co/ZrO_2 exhibited the lowest adsorption capacity of 2,4-D and the highest activity for catalytic ozonation of TOC removal at neutral conditions. The results suggested that the 2,4-D degradation at neutral pH values should only come from the reaction with free oxygen radical species in solution. While the TOC removal at pH = 4.0 should be attributed to the adsorption of 2,4-D onto Fe–Co/ZrO_2.

Figure 8 showed the effect of co-existing anions on the ozonation efficiency of 2,4-D over Fe–Co/ZrO_2. The results indicated that the ozonation efficiency was greatly inhibited in the presence of anions (curve e) compared with that when anion was absent or present alone. Moreover, PO_4^{3-} inhibited the catalytic activity of Fe–Co/ZrO_2 more significantly than HCO_3^- and SO_4^{2-}. It seems that some interaction between the catalyst and anions occurred, which suppressed the ozone decomposition into oxygen radical species.

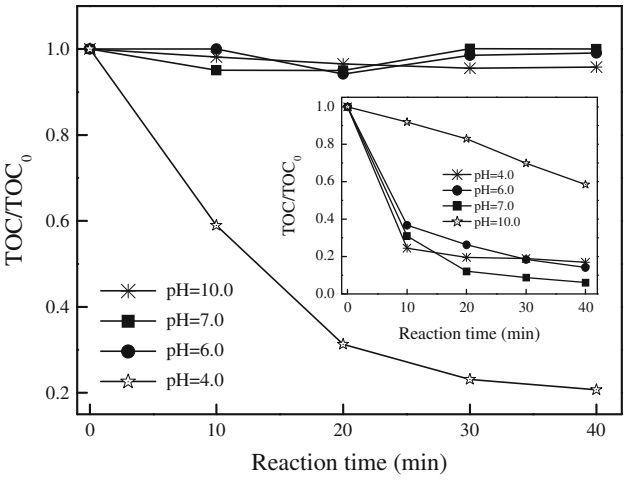

Fig. 7 Effect of solution pH on the 2,4-D (50 mg/L) adsorption over Fe–Co/ZrO_2 and the TOC removal (inset) over Fe–Co/ZrO_2 with ozone (catalyst = 2.0 g/L, gas ozone concentration = 30 mg/L)

3.4 Catalytic Ozonation Mechanism

It is necessary to investigate the catalytic mechanism of pollutants degradation over Fe–Co/ZrO_2 with ozone. Catalytic ozonation could decompose ozone more effectively than ozonation alone (Fig. 9). Moreover, the ozone decomposition rate was accelerated in the presence of PO_4^{3-}. Since 40 % of PO_4^{3-} was adsorbed on the surface of Fe–Co/ZrO_2 and PO_4^{3-} was a harder Lewis base [2], the existence of PO_4^{3-} could poison the catalyst (the active sites in Fe–Co/ZrO_2 was Lewis acids). As shown in Fig. 10, there was no significant difference between the spectra of catalyst suspensions with/without ozone. However, the absorption band of hydrogen-bonded MeO–H disappeared in the presence of PO_4^{3-}, while two new peaks

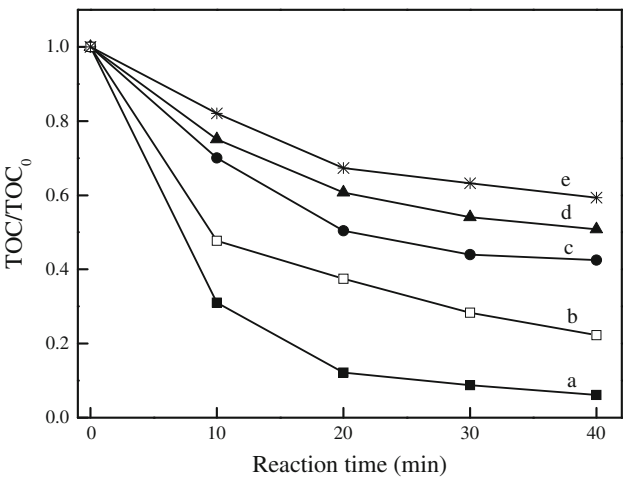

Fig. 8 Effect of co-existing anions (2.0 mM) on the TOC removal of 2,4-D solution (50 mg/L) over Fe–Co/ZrO_2 with ozone: *a* without anions, *b* SO_4^{2-}, *c* HCO_3^-, *d* PO_4^{3-}, *e* SO_4^{2-} + HCO_3^- + PO_4^{3-} (pH = 7.0, catalyst = 2.0 g/L, gas ozone concentration = 30 mg/L)

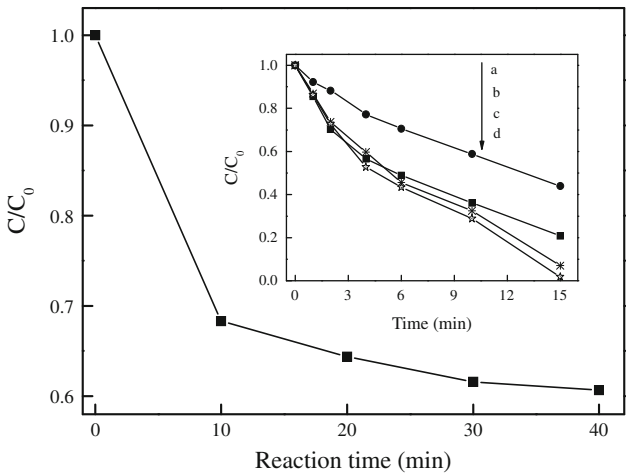

Fig. 9 Adsorption of PO_4^{3-} on Fe–Co/ZrO_2 and decomposition of ozone (inset) at pH = 7.0 under different conditions: *a* ozone alone, *b* ozone with PO_4^{3-}, *c* ozone with Fe–Co/ZrO_2, *d* ozone with Fe–Co/ZrO_2 and PO_4^{3-}

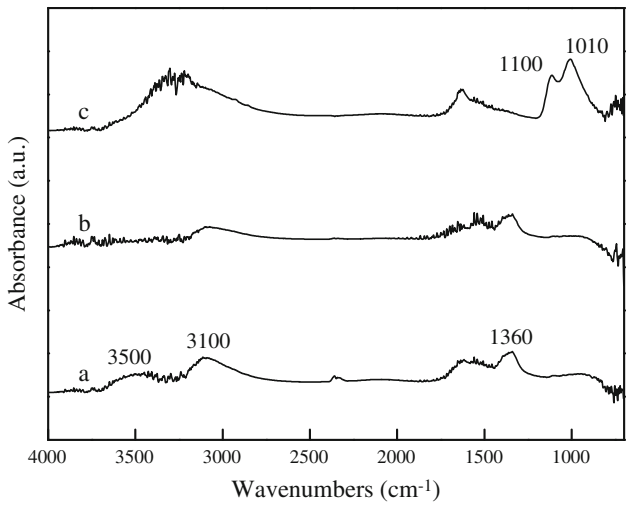

Fig. 10 ATR-FTIR spectra of Fe–Co/ZrO_2 suspension: *a* catalyst, *b* catalyst + O_3, *c* catalyst + PO_4^{3-} + O_3

at 1,010 and 1,100 cm^{-1} belonging to PO_4^{3-} vibrations appeared. The studies of in situ ATR-FTIR supplied direct evidences for the presence of PO_4^{3-} on the surface of Fe–Co/ZrO_2.

PO_4^{3-} in solution then played two roles in influencing the reactivity of Fe–Co/ZrO_2. One is that PO_4^{3-} held the surface Lewis acid sites on the catalyst, which prevented the chemisorption of ozone, leading to the lower efficiency of ozone decomposition into oxygen radical species. Besides, the decomposition of ozone belonged to the chain reaction, producing free radicals, which could be scavenged by anions and organic [2, 26], thus accelerating the ozone decomposition. The other role of PO_4^{3-} was then to trap oxygen radical species by competing with pollutant. Therefore, the presence of PO_4^{3-} would result in the decrease of TOC removal efficiency (Fig. 8).

According to the above experiments and previous literature [2, 3], a possible mechanism for the catalytic ozonation of pollutants over Fe–Co/ZrO_2 was proposed. The chemisorbed ozone was catalytically transformed into $^{\bullet}OH$ by Fe–Co oxides, which react with non-chemisorbed organic molecule in water. The interfacial electron transfer was involved in the catalytic decomposition reaction of ozone. The multivalence of Fe–Co oxides have two redox couples (Fe^{3+}/Fe^{2+} and Co^{2+}/Co^{3+}) to form galvanic cells and enhance the electron transfer, resulting in higher activity for the mineralization of toxic pollutants. Therefore, the dispersion and multivalent oxidation state of the supported Fe–Co oxides were crucial factors for the high efficiency of the catalytic ozonation.

4 Conclusions

Fe–Co oxides were highly dispersed on the surface of mesoporous zirconia with multivalent oxidation states by incipient wetness co-impregnation method. Compared with individual component Fe or Co catalysts, Fe–Co/ZrO_2 exhibited higher ozonation efficiency for the degradation of the tested toxic pollutants such as 2,4-D, PZ and DP in aqueous solution. The multivalent oxidation states, high dispersion and the synergistic effect of Fe–Co oxides in the catalyst enhanced the interfacial electron transfer process, which caused the higher catalytic reactivity for ozone decomposition into $^{\bullet}OH$ radicals, leading to the efficient removal of toxic pollutants in aqueous solution.

Acknowledgments This work was financially supported by the NSFC (Nos. 50921064, 20977104, 50908223) and the 973 project (No. 2010CB933604).

References

1. Schwarzenbach RP, Escher BI, Fenner K, Hofstetter TB, Johnson CA, von Gunten U, Wehrli B (2006) Science 313:1072
2. Kasprzyk-Hordern B, Ziolek M, Nawrocki J (2003) Appl Catal B 46:639
3. Nawrocki J, Kasprzyk-Hordern B (2010) Appl Catal B 99:27
4. Benner J, Ternes TA (2009) Environ Sci Technol 43:5086
5. Song S, Liu ZW, He ZQ, Zhang AL, Chen JM, Yang YP, Xu XH (2010) Environ Sci Technol 44:3913
6. Sui MH, Sheng L, Lu KX, Tian F (2010) Appl Catal B 96:94
7. Yang L, Hu C, Nie YL, Qu JH (2009) Environ Sci Technol 43:2525
8. Einaga H, Futamura S (2004) React Kinet Catal Lett 81:121
9. Wojciechowska M, Zielinski M, Malczewska A, Przystajko W, Pietrowski M (2006) Appl Catal A 298:225
10. Wang HL, Yang Y, Xu J, Wang H, Ding MY, Li YW (2010) J Mol Catal A 286:29

11. Bokare AD, Chikate RC, Rode CV, Paknikar KM (2008) Appl Catal B 79:270
12. Raja R, Hermans S, Shephard DS, Johnson BFG, Raja R, Sankar G, Bromley S, Thomas JM (1999) Chem Commun 16:1571–1572
13. Wang JJ, Chernavskii PA, Khodakov AY, Wang Y (2012) J Catal 286:51
14. Logdberg S, Tristantini D, Borg O, Ilver L, Gevert B, Jaras S, Blekkan EA, Holmen A (2009) Appl Catal B 89:167
15. Lee CH, Sedlak DL (2008) Environ Sci Technol 42:8528
16. Reddy BM, Rao KN, Bharali P (2009) Ind Eng Chem Res 48: 8748
17. Liu LJ, Chen Y, Dong LH, Zhu J, Wan HQ, Liu B, Zhao B, Zhu HY, Sun KQ, Dong L, Chen Y (2009) Appl Catal B 90:105
18. Liu XM, Lu GQ, Yan ZF (2004) J Phys Chem B 108:15523
19. Bader H, Hoigne J (1981) Water Res 15:449
20. Li XQ, Zhang WX (2006) Langmuir 22:4638
21. Nie YL, Hu C, Qu JH, Zhao X (2009) Appl Catal B 87:30
22. Li FB, Li XZ (2002) Appl Catal A 228:15
23. Vetrivel S, Pandurangan A (2005) J Mol Catal A 227:269
24. Somanathana T, Pandurangana A, Sathiyamoorthy D (2006) J Mol Catal A 256:193
25. Hu C, Xing ST, Qu JH, He H (2008) J Phys Chem C 112:5978
26. Lv AH, Hu C, Nie YL, Qu JH (2010) Appl Catal B 100:62